

26 May 2010, 4:45 pm - 6:45 pm

## Effect of Liquefaction on Pile Shaft Friction Capacity

M. E. Stringer  
*University of Cambridge, U.K.*

S. P. G. Madabhushi  
*University of Cambridge, U.K.*

Follow this and additional works at: <https://scholarsmine.mst.edu/icrageesd>



Part of the [Geotechnical Engineering Commons](#)

---

### Recommended Citation

Stringer, M. E. and Madabhushi, S. P. G., "Effect of Liquefaction on Pile Shaft Friction Capacity" (2010). *International Conferences on Recent Advances in Geotechnical Earthquake Engineering and Soil Dynamics*. 16.  
<https://scholarsmine.mst.edu/icrageesd/05icrageesd/session05/16>



This work is licensed under a [Creative Commons Attribution-Noncommercial-No Derivative Works 4.0 License](#).

This Article - Conference proceedings is brought to you for free and open access by Scholars' Mine. It has been accepted for inclusion in International Conferences on Recent Advances in Geotechnical Earthquake Engineering and Soil Dynamics by an authorized administrator of Scholars' Mine. This work is protected by U. S. Copyright Law. Unauthorized use including reproduction for redistribution requires the permission of the copyright holder. For more information, please contact [scholarsmine@mst.edu](mailto:scholarsmine@mst.edu).



Fifth International Conference on

## Recent Advances in Geotechnical Earthquake Engineering and Soil Dynamics and Symposium in Honor of Professor I.M. Idriss

May 24-29, 2010 • San Diego, California

### **EFFECT OF LIQUEFACTION ON PILE SHAFT FRICTION CAPACITY**

**M.E. Stringer**

Department of Engineering, University of Cambridge  
Cambridge, United Kingdom

**S.P.G. Madabhushi**

Department of Engineering, University of Cambridge  
Cambridge, United Kingdom

#### **ABSTRACT**

Piled foundations are commonly used worldwide, and observed failures of these foundations during earthquakes has led to active research in this area. However, the way in which piles support axial loads during earthquakes is still not fully understood. In this paper, the results from centrifuge tests are presented which consider how axial loads are carried by piles during earthquake loading. It will be shown that the piles in dry soils mobilise additional shaft friction to carry the seismically induced axial loading. However, in the case of a pile group passing through a liquefiable soil layer and founded in a dense sand layer, the pile group suffered large settlements as it loses the shaft friction in the liquefied layer and attempted to mobilise additional end bearing capacity. Further, with the post-seismic dissipation of pore pressures and the consequent settlement of the soil, the piles register significant down drag forces. This resulted in a reduction of the loads being supported as shaft friction and required further end bearing capacity to be mobilised.

#### **INTRODUCTION**

Piled foundations have become popular worldwide as a solution for transferring high structural loading through weak or compliant soil layers to stiffer or more competent soils below the surface. However, during earthquake events, liquefaction of surrounding soils has led to many failures, especially lateral spreading occurs and soil flows past the piled foundation. In the case of bridges, the effects of failure are not limited to the damage caused to the bridge itself. After an earthquake, access to the affected areas is of great importance as it can often be a key factor in the event's ultimate toll. The failure of piled foundations during earthquakes has therefore led to active research in this area. Much of the research carried out in this area has focussed on the bending moments exerted on the piles during lateral spreading, for example Abdoun et al. (2003) and Brandenberg et al. (2005). However, some research has been carried out to investigate some alternative modes of failure. Bhattacharya et al. (2005) investigated the axial failure of single rock-socketed piles in liquefiable soils, finding if sufficiently loaded, these pile foundations were prone to buckling as the lateral soil support reduced. This work has been extended by Knappett and Madabhushi (2009), who showed that pile groups are also

subject to unstable collapse if the axial load is sufficiently high. However, the preceding two works rely on the high vertical support provided by the base rock. In the case of most piles, the bedrock is located too deep for piles to be able to realise the rock-socketed condition. Knappett & Madabhushi (2008) carried out centrifuge tests to investigate the behaviour of pile groups which passed through a liquefiable deposit into a dense bearing layer. These tests showed that the onset of liquefaction led to softening of the system's vertical stiffness and therefore significant settlement occurred. However, despite the research on piled foundations in liquefiable soils, there remains a fundamental lack of knowledge surrounding the manner in which a piled foundation is able to carry loads during the earthquake.

Pile groups are able to carry their applied axial loads as a combination of end bearing, shaft friction and pile cap bearing. In the presence of an air gap beneath the pile cap, the pile cap bearing capacity will be zero until the point where the pile group comes into contact with the ground, where after it can mobilise some pile cap bearing capacity. The axial loading on a pile is shown in Figure 1.

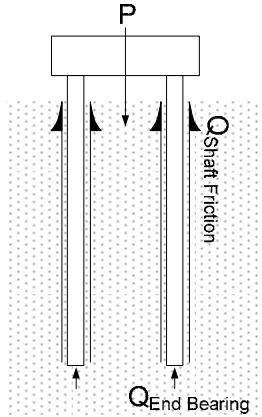


Figure 1: Axial Loading

In this paper a series of centrifuge experiments is presented which considers at the differing shaft friction response in liquefiable and non-liquefied soils

## CENTRIFUGE MODELLING

### Preparation

Two dynamic centrifuge experiments, MS1 & MS2 were carried out at 80g using the beam centrifuge at the University of Cambridge. In both cases, a 2x2 pile group was inserted into a two layer sand profile where a dense layer of coarse sand was overlain by a loose layer of fine sand.

Table 1: Sand Properties

Parameter	Fraction E Sand	Fraction C Sand
$D_{10}$	0.110mm	0.442mm
$D_{50}$	0.174mm	0.590mm
$e_{min}$	0.613	0.491
$e_{max}$	1.014	0.829
$\phi_{crit}$	33	31

An automatic sand pourer, described by Zhao et al. (2006), was used to create the dense layer. Fraction C silica sand was used in this layer, and was poured with relative density,  $D_r = 100\%$ . The loose, liquefiable layer used Fraction E silica sand using a manual overhead sand hopper, achieving a relative density of approximately 35%. In both cases, pouring was

interrupted to allow the placement of pore pressure transducers and accelerometers by hand. Selected properties for the two sands are given in Table 1. Since the permeability of a soil is linked to the square of the  $D_{10}$  grain size, the dense layer of Fraction C sand is expected to have a significantly higher permeability than the overlying loose layer of Fraction E sand.

In the case of MS1, after sand pouring was completed, the model was placed under vacuum and fully saturated using a computer controlled system, described by Stringer & Madabhushi (2009). A solution of Methyl Cellulose with a viscosity of 80cSt was used for the pore fluid and corrects for the discrepancy in time scaling discussed by Schofield (1981). Test MS2 was conducted in the unsaturated condition.

Prior to spin-up, the pile group was driven into the model at 1-g, and time allowed for any pore pressures to dissipate. Since the primary interest in these experiments was the shaft friction response of the piles, an air gap was left below the pile cap to ensure that loads could only be supported as a combination of end bearing pressure and shaft friction. The 2x2 pile group is fully described by Knappett (2006), while important parameters are reproduced in Table 2. Aluminium blocks were rigidly attached to the top of the pile cap in order to apply axial load to the piles. The blocks used resulted in an axial load per pile of approximately 450kN at prototype scale.

Table 2: Important pile parameters

Parameter	Nomenclature	Value (prototype)
Outer Diameter	$D_0$	0.496m
Pile Spacing	$s$	2.8m
Embedded Length	$L_p$	15.4m
Bending Stiffness	$EI$	164MNm <sup>2</sup>
Axial Stiffness	$EA/L_p$	0.96MN/m

### Model Layout

The model layouts used in MS1 and MS2 are shown in Figure 2. Pore pressure transducers (PPT) and accelerometers were placed in the soil to observe soil response. The pile group's settlement was measured using two draw wire potentiometers, which were located on opposite sides of the pile group, which were normal to the direction of shaking. Pile cap accelerations in the direction of shaking were measured using an accelerometer which was rigidly attached to the side of the pile cap.

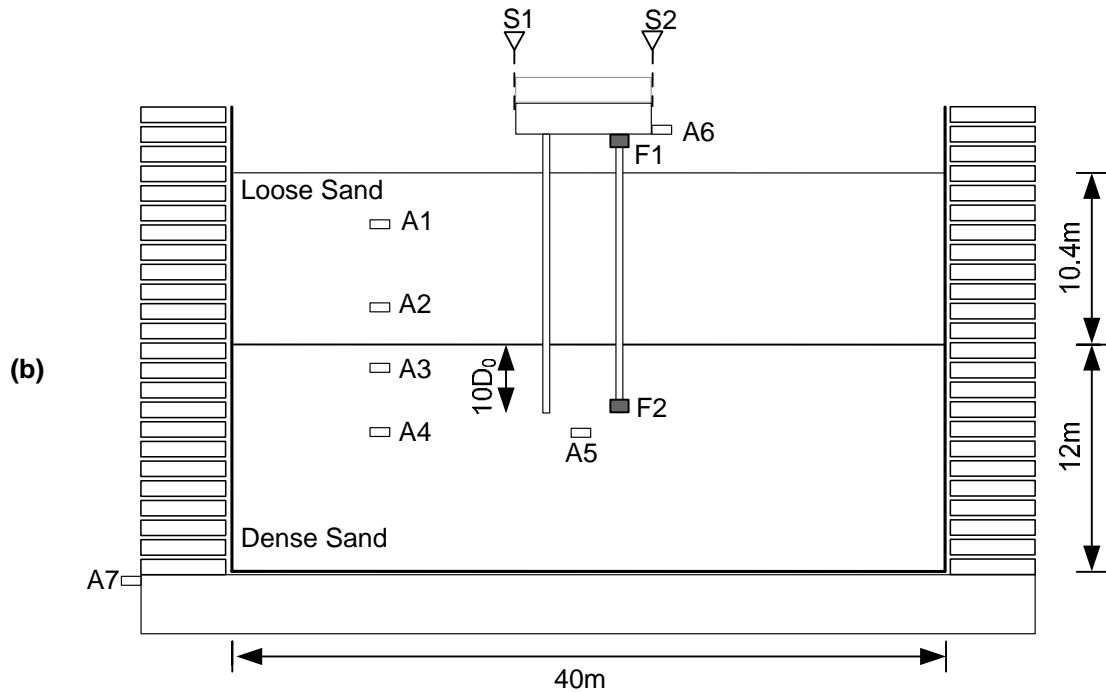
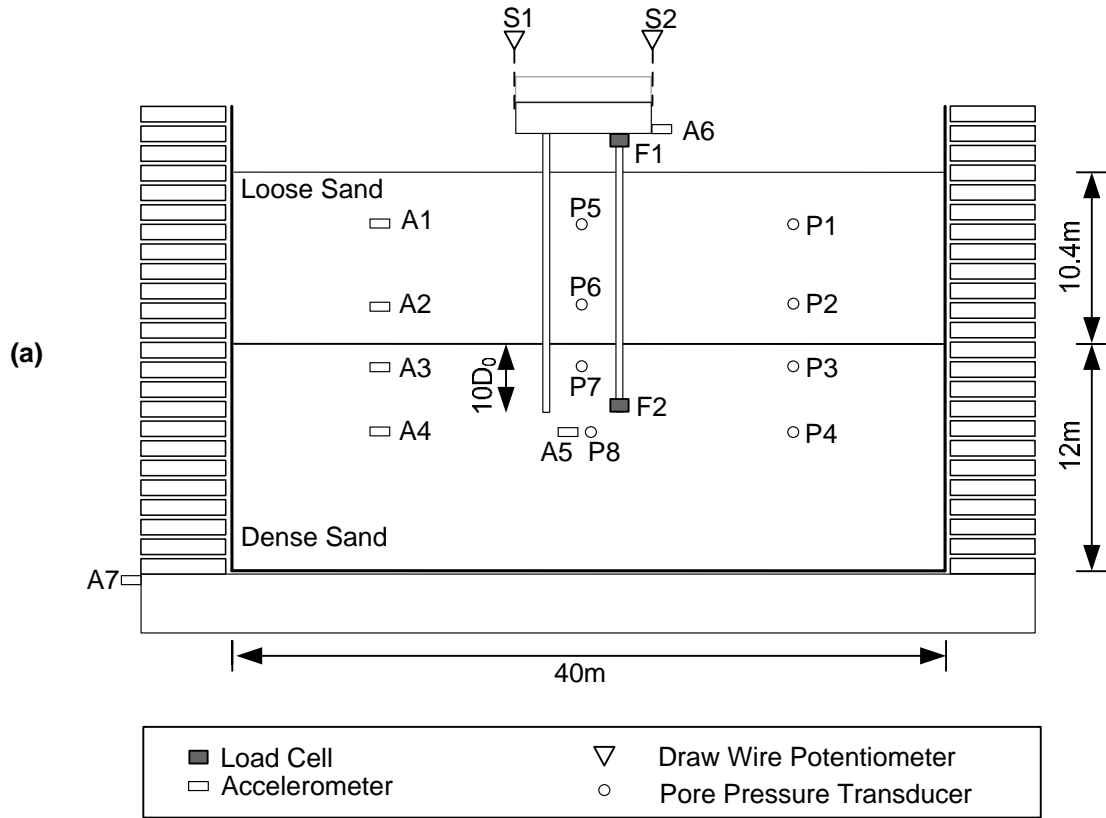


Figure 2: Cross Section of centrifuge models, dimensions shown in prototype scale. a) MS1 b) MS2

## Testing

Data from the instruments was recorded in both the swing-up phase and the earthquake phase of the test. During swing-up, data was logged at 4Hz. The sampling rate was increased to 4kHz while the earthquake was fired, and then reduced to 10Hz in the post-earthquake phase while pore pressures dissipated.

In both tests, simple earthquake shaking was applied to the models using the stored angular momentum (SAM) actuator, described by Madabhushi et al. (1998). The applied model earthquakes were 30 cycles of roughly sinusoidal motion, with a fundamental frequency of 0.63Hz and peak amplitude of 0.18g at prototype scale.

It was observed during swing up that the load applied at the top of the instrumented pile was close to a quarter of the expected total cap load, indicating that the load was spread evenly on the piles.

## RESULTS

The data collected during testing has been passed through a low pass filter at 500Hz (model scale) and is presented in this paper in prototype scale.

### Liquefaction during MS1

The excess pore pressures which were recorded in the free field during the shaking are shown in Figure 3 (a-b) with the dashed lines showing the excess pore pressures required to cause full liquefaction at that depth. It is clear that the earthquake loading was strong enough to cause full liquefaction throughout the loose layer. Close to the top of the dense layer, pore pressures are also high enough to reach liquefaction briefly once a cycle, as a result of the high pore pressures in the overlying loose layer. Lower in the dense layer, excess pore pressures are clearly being generated, but to a lesser extent such that the pore pressures do not rise high enough to cause full liquefaction. The excess pore pressures recorded by PPTs P3 and P4 are seen to begin dissipating during the earthquake due to the high permeability of the dense layer.

After the earthquake loading ends, rapid equalisation of excess pore pressures occurs throughout the dense layer, due to the high permeability of the soil layer. However, in the loose layer, it is seen that the pore pressures take much longer to dissipate, since the permeability of this layer is much lower. Although the pore pressures in the dense layer equalise rapidly after shaking, they are then constrained to remain at the level

of excess pore pressures at the base of the loose layer. This results in a much lower rate of excess pore pressure dissipation after the initial equalisation and a much slower build-up of effective stresses than would otherwise be observed in this type of soil.

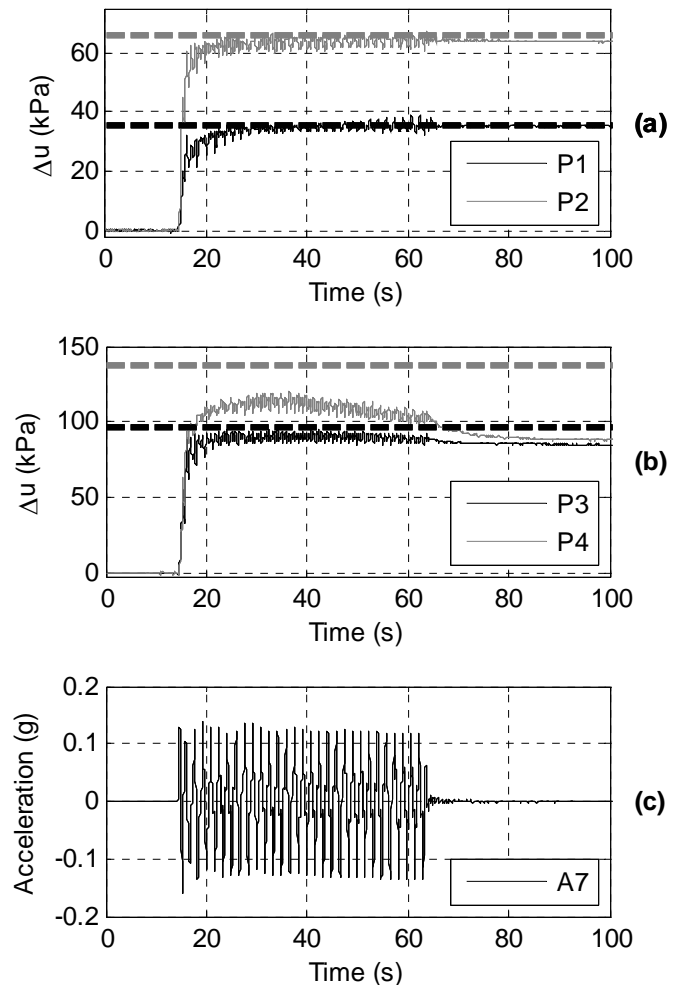


Figure 3: Pore pressures in the free field during MS1: a) loose layer, b) dense layer; c) input acceleration

### Behaviour in Liquefied Sand

The loading recorded by the pile cap during MS1 is shown in Figure 4. The loading applied at the top of the pile is seen to oscillate at the fundamental frequency with the magnitude cycling about the static pile load value. The cyclic loading at the pile head is due to the pile group rocking during shaking. At the start of the shaking, the load measured at the top of the pile is seen to be greatest. Similarly, the pile cap acceleration is seen to be largest at the beginning of the earthquake, where it is amplified by a factor of approximately 2. However, as

shaking progresses, the amplification factor reduces quickly until it reaches a value of 0.5 after 5 cycles. It was seen in Figure 3 that full liquefaction is reached after 5 cycles and free field acceleration records show that the accelerations in the loose soil layer become highly attenuated after a couple of cycles. Both of these observations show that the surrounding soil is greatly softened during the liquefaction and as a result, the input motion is not being transferred effectively to the pile cap. The cyclic variation in load applied at the pile cap is due to the rocking motion of the pile group caused by the input accelerations. Since the pile cap acceleration is greatly reduced as the surrounding soil softens, the recorded cyclic loading at the pile head correspondingly reduces with the onset of liquefaction.

The change in load recorded at the pile tip is shown in Figure 4(b). It is clear that the end bearing load cycles at the fundamental frequency and with a magnitude of cyclic variation similar to that of the applied loading. Examination of the end bearing load and the applied loading also revealed that these two quantities were close to being in phase, with the end bearing load only slightly lagging the applied tip loading. The cycle averaged end bearing load is seen to increase at the very start of the shaking, but then drops until 9 cycles into the shaking, where it again begins to increase. It is seen in Figure 4 that in the period when end bearing load is decreasing, the rate of settlement with time is increasing, suggesting downward acceleration. However, after approximately 9 cycles of shaking, the rate of settlement with time starts to decrease, suggesting that the pile cap is decelerating slightly in the downward direction.

It is observed that the pile group begins to settle as soon as shaking is applied. The settlement continues to increase throughout the duration of the earthquake, with large final settlements of nearly 600mm being recorded ( $1.2D_0$ ). It is also clear from Figure 4 that the settlements cease at the same instant that the shaking ends. The co-seismic settlements, recorded by S1 and S2, have a strong cyclical element at the shaking frequency and cycle out of phase to each other. In each cycle, both S1 and S2 show a step increase in settlement, followed by a plateau. This agrees with the mechanism proposed by Knappett (2008b), in which the pile cap rocks from side to side and each leg “stomps” its way into the soil.

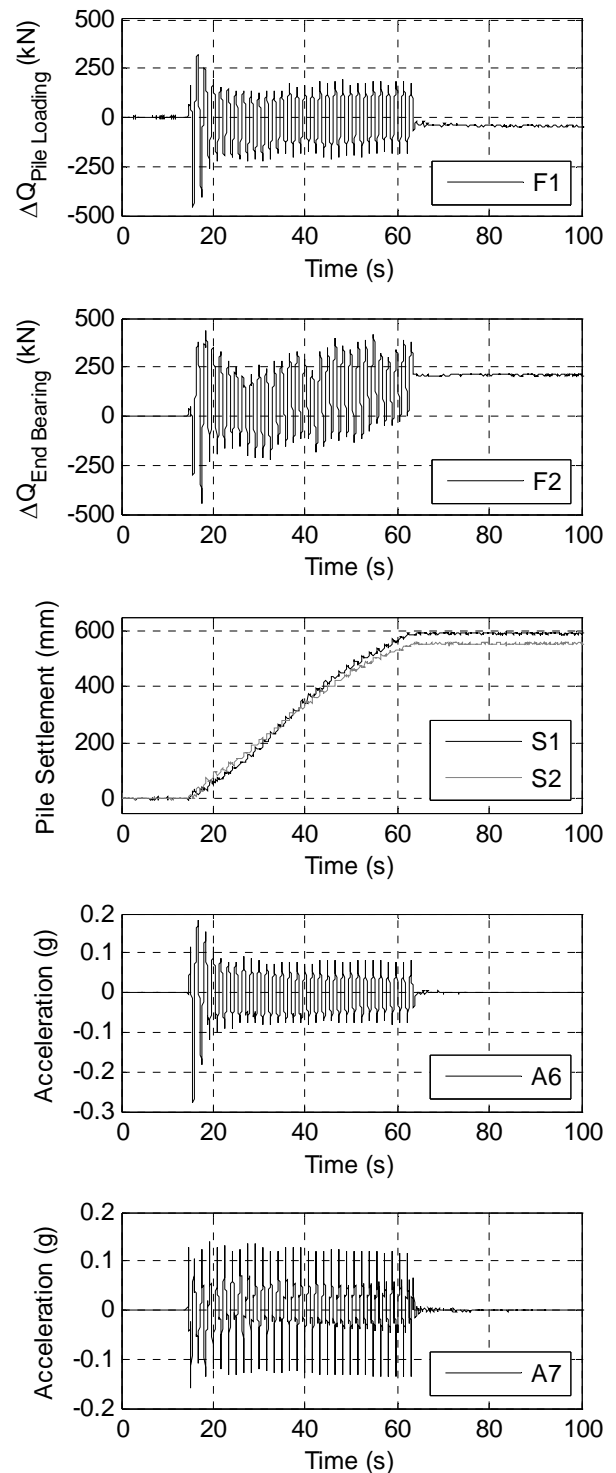


Figure 4: Pile Group Loading and Settlement during MS1

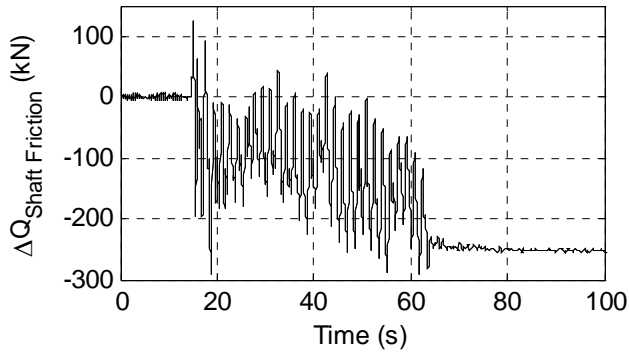


Figure 5: Average Shaft Friction during MS1

The changes in shaft friction during MS1 have been calculated as the difference between the load applied to the pile and the load carried as end bearing. The change in shaft friction has been plotted in Figure 5. It is seen on the figure that the magnitude of the cyclic changes in shaft friction are much lower than either of those recorded for the end bearing load or the applied loads. Further, it is clear when Figure 4 and Figure 5 are compared that the shaft friction leads the applied pile loading & the end bearing load by significant amounts. It was also found that the phase leads were significantly different depending on whether the pile loading was increasing or decreasing. In the case a local maximum in shaft friction, the phase lead was approximately  $150^\circ$  whereas at local minimums, the phase lead was reduced to approximately  $100^\circ$ .

#### Behaviour in Unsaturated Sand

A second test, with similar layout to MS1 was carried out in the unsaturated condition, with similar input accelerations. The results from this test are shown in Figure 6.

Figure 6 (d) shows the accelerations recorded on the pile cap. It is seen that the pile cap acceleration is amplified relative to the base input, which is shown in Figure 6 (e). Unlike the pile cap accelerations in MS1, the amplification of pile cap accelerations increases gradually through the earthquake loading. The pile cap accelerations appear to cycle at double the fundamental frequency. When the pile cap acceleration was compared with the input acceleration in the frequency domain, it became clear that the pile cap was exhibiting resonance at a frequency of approximately 1.75Hz.

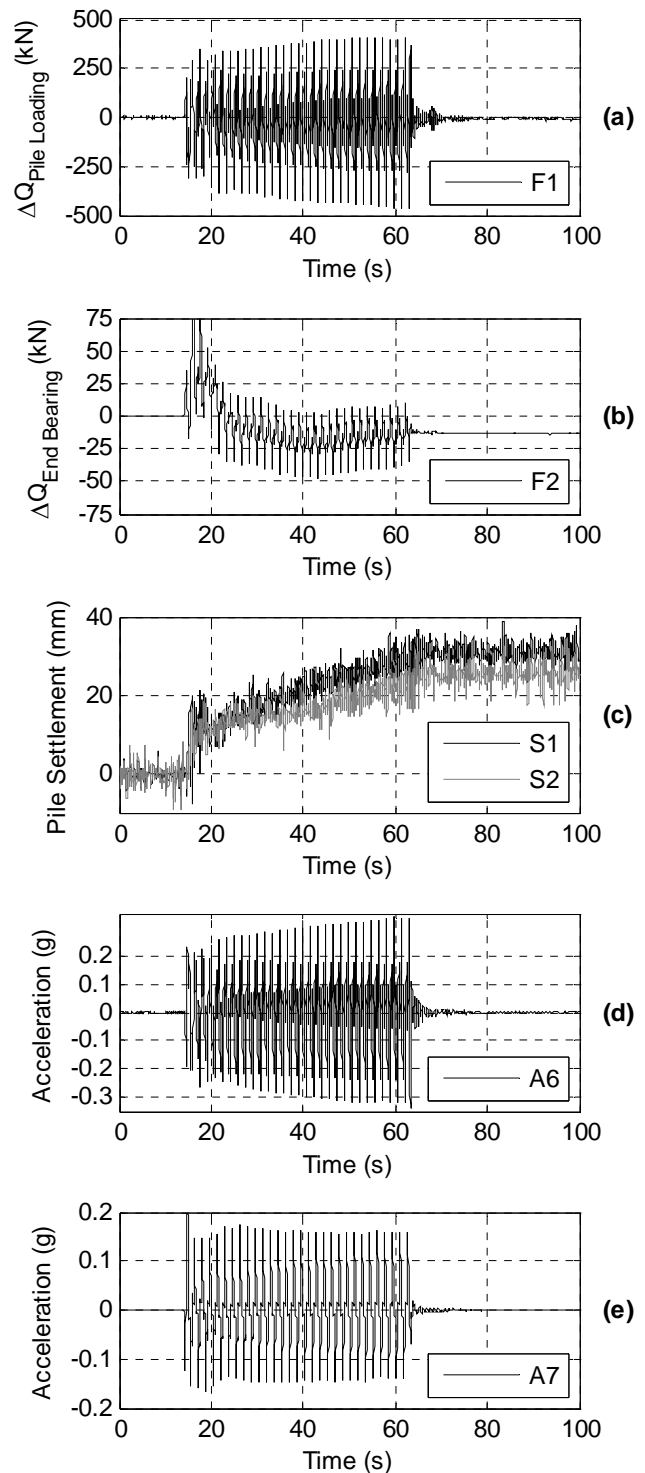


Figure 6: Pile Group Loading & Settlement in MS2

Similar to MS1, the loads recorded at the pile head follow the same patterns as the pile cap acceleration. At the pile tip, an initial increase in end bearing load is observed, but this quickly reduces and cycles close to its original load. Despite the pile head load showing a strong component at the first harmonic of the fundamental frequency, the load recorded at the pile tip predominantly cycles at the fundamental frequency. The magnitude of the cyclic loading is also noticeably small when compared with the load applied at the pile head.

The pile group was seen to accumulate close to 1/3 of its total settlement at the beginning of the earthquake loading, increasing gradually thereafter to a total settlement of 30mm (0.06D<sub>0</sub>). Similar to MS1, settlement ceased to accumulate once shaking ends.

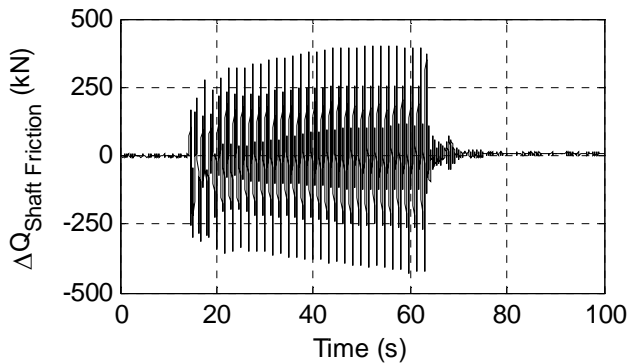


Figure 7: Changes in shaft friction during MS2

The shaft friction during MS2 is shown in Figure 7. The changes in pile shaft friction in this test is seen to be very similar to the pile head loading, due to the relatively small changes in the loads measured at the pile tips.

#### Post-seismic behaviour.

In both MS1 and MS2, the pile group ceased to accumulate any further settlements after the shaking had ended. In a dry test, this is expected, since the capacity of the foundation should be similar to that before the earthquake. However, in MS1, where the soil was saturated, the excess pore pressures which were generated during the shaking must dissipate before the effective stresses can return to their pre-shaking values. This would imply a period after shaking where the piles would be expected to settle further, in direct contrast to the experimental results and suggests that the settlement observed during the earthquake is not solely a function of the reduced effective stresses in the model.

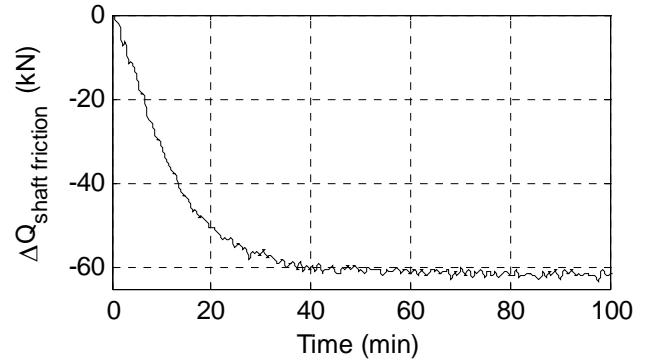


Figure 8: Post-seismic change in average shaft friction in MS1

The change in post-seismic shaft friction is shown in Figure 8. In the period from 0 min to approximately 50 minutes, the pore pressures are dissipating. The shaft friction which can be mobilised is linked to the effective stress and therefore the shaft friction capacity in this period is increasing. However, the records show that the proportion of load being carried in shaft friction is decreasing during this period. Since the pile cap is not in contact with the soil surface, no load can be carried as raft pressure and therefore more load is transferred to end bearing. This increase in end bearing is shown in Figure 9, where it is plotted against the dissipation of excess pore pressures recorded by P8. The figure shows a very strong correlation between these two parameters.

Since the pile is not settling further, the soil directly beneath the piles is stiff enough to resist further settlement after shaking. As the excess pore pressures dissipate, the soil beneath the pile tips must be gaining further strength and stiffness faster than the end bearing load is increasing. The strong correlation between the change in excess pore pressure and the end bearing load suggests that soil down drag on the pile is responsible for the observed reduction in shaft friction. Shaft friction is positive when the soil is supporting the pile, therefore if the soil next to the pile settles, while the pile itself is not settling, this will manifest its self as the shaft friction decreasing, or possibly even becoming negative if the soil settles far enough.



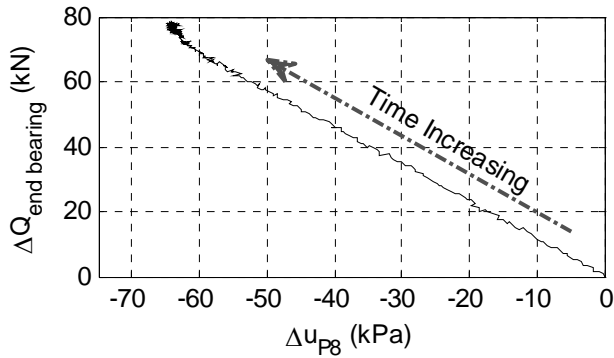


Figure 9: Post-seismic change in end bearing load against excess pore pressure in MS1

No change in the post seismic shaft friction was observed in MS2, where the soil was not saturated, as would be expected if the decrease in shaft friction after an earthquake is linked to soil consolidation.

## DISCUSSION

In the previous section, it was seen that accelerations measured at the pile cap are very different depending on whether the surrounding soil is able to liquefy or not. In the case of the former, the degradation of the soil stiffness leads to much lower accelerations being transferred to the pile group and therefore much lower shear loads at the top of the piles. However, the pile group still experiences strong accelerations in the first couple of cycles of the earthquake loading and must therefore still be able to resist significant shear loading, similar to the pile group located in unsaturated sand.

The changes in shaft friction derived from measurements of axial load at the top and bottom of the pile during the earthquake loading showed different behaviour during the unsaturated and saturated tests. Assuming that the shaft friction mobilisation distance is small, then three different shaft friction responses might be observed depending on whether the full capacity is reached each cycle. If the full shaft friction capacity is not being reached, then almost all of the applied pile head loading will be carried in shaft friction, with only a small amount of the pile head loading being transferred to the base due to the pile settling in order to mobilise the extra shaft friction. This scenario was seen in the dry test. A second situation exists where the applied pile head loading is greater than the shaft friction capacity of the pile. In this case, the applied pile head load is initially taken in shaft friction, until the shaft friction capacity is exceeded, whereafter further pile head loading is transferred to the base of the pile. Since the load is initially taken as shaft friction, then the shaft friction will lead the applied pile head load, with

the phase lead increasing with the proportion of load transferred to end bearing. This scenario appears to match what was observed in the saturated test, MS1. A third situation exists if the pile shaft friction capacity is reduced to zero. In this case, all the applied pile head load must be supported in end bearing.

The preceding discussion assumed that the mobilisation distance for the shaft friction was small. However, if this is not the case, and there is a significant mobilisation distance, then it is possible that the full shaft friction of the pile is not achieved, but that some load transfer occurs to the base of the pile due as the pile settles and attempts to mobilise extra shaft friction capacity. Under this scenario, both the changes in pile shaft friction and pile end bearing would cycle in phase with the pile head load.

## CONCLUSIONS

The manner in which piles sustain the axial loading during an earthquake has been shown to be significantly affected by the onset of liquefaction. In the case where liquefaction was observed, the load carried as shaft friction dropped substantially during the earthquake loading. Soil down drag after the earthquake resulted in further load transfer to the pile tips, requiring additional end bearing capacity to be mobilised. In order to mobilise the additional required end bearing capacity, the pile group was observed to suffer extensive settlement.

Where the ground was unsaturated, it was found that the pile was able to sustain the cyclic axial loading by mobilising extra shaft friction capacity, with little load being transferred to the base of the pile. Since the pile was able to carry the earthquake-induced pile head loads in shaft friction, no extra base capacity needed to be mobilised and therefore much more modest settlements were observed compared with the saturated case with soil liquefaction.

The accelerations of the superstructure were observed to attenuate quickly with the onset of liquefaction as the surrounding soil liquefied, leading to lower lateral forces being transmitted to the piles. In the unsaturated soil however, the accelerations were not attenuated as the earthquake loading progressed and so the lateral loads applied to the piles remain high for the entirety of the earthquake.

## ACKNOWLEDGEMENTS

The first author would like to acknowledge the financial support of the Engineering and Physical Sciences Research Council, UK.

## REFERENCES

Abdoun, T., Dobry, R., O'Rourke, T.D. & Goh, S.H. [2003]. "Pile response to lateral spreads: centrifuge modeling", *J. Geotechnical and Geoenvironmental Engineering*, Vol. 129, No. 10, pp 869-878

Bhattacharya, S, Madabhushi, S.P.G. & Bolton, M.D. [2005]. "An alternative failure mechanism of pile failure in liquefiable deposits during earthquakes", *Geotechnique*, Vol. 54, No. 3, pp 259-263

Brandenberg, S.J., Boulanger, R.W., Kutter, B.L. & Chang, D. [2005]. « Behaviour of pile foundations in laterally spreading ground during centrifuge tests", *J. Geotechnical and Geoenvironmental Engineering*, Vol. 131, No. 11, pp 1378-1391

Knappett, J.A. [2006]. "Piled foundations in liquefiable soils: Accounting for axial loads", PhD Thesis, University of Cambridge, UK

Knappett, J.A. & Madabhushi, S.P.G. [2008a]. "Liquefaction-induced settlement of pile groups in liquefiable and laterally spreading spreading soils", *J. Geotechnical and Geoenvironmental Engineering*, Vol. 134 No. 11, pp 1609-1618

Knappett, J.A. & Madabhushi, S.P.G. [2008b]. "Mechanism of pile group settlement in liquefiable soils," *Proc. Geotechnical Earthquake Engineering and Soil Dynamics*, Sacramento, United States

Knappett, J.A. & Madabhushi, S.P.G. [2009]. "Influence of axial load on lateral pile response in liquefiable soils. Part I: physical modelling", *Geotechnique*, Vol 59, No. 7, pp 571 - 581

Madabhushi, S.P.G., Schofield, A.N. & Lesley, S. [1998]. "A new stored angular momentum based earthquake actuator", *Proc. Centrifuge '98*, Tokyo, Japan, Vol.1, pp111-116

Schofield, A.N. [1981]. "Dynamic and earthquake geotechnical centrifuge modelling", *Proc. International Conference on Recent Advances in Geotechnical Earthquake Engineering and Soil Dynamics*, St. Louis, USA, Vol.3 pp1081 – 1100

Stringer, M.E. & Madabhushi, S.P.G. [2009]. "Novel computer-controlled saturation of dynamic centrifuge models using high viscosity fluids", *Geotechnical Testing Journal*, Accepted for publication Aug. 2009

Zhao, Y., Gafar, K., Elshafie, M.Z.E.B., Deeks, A.D., Knappett, J.A. & Madabhushi, S.P.G. [2006]. "Callibration

and use of a new automatic sand pourer", *Proc. Int. Conf. on Physical Modelling in Geotechnics*, Hong Kong, pp 265-270